Fibrotic and Vascular Remodelling of Colonic Wall in Patients with Active Ulcerative Colitis

Journal of Crohn's and Colitis Advance Access published March 19, 2016

Manuscript Doi : 10.1093/ecco-jcc/jjw076

Fibrotic and Vascular Remodelling of Colonic Wall in Patients with Active Ulcerative Colitis

Chiara Ippolito,[a] Rocchina Colucci,[b] Cristina Segnani,[a] Mariella Errede,[c] Francesco Girolamo,[c] Daniela Virgintino,[c] Amelio Dolfi,[a] Erika Tirotta,[b] Piero Buccianti,[d] Giulio Di Candio,[d] Daniela Campani,[e] Maura Castagna,[e] Gabrio Bassotti,[f] Vincenzo Villanacci,[g] Corrado Blandizzi,[b] Nunzia Bernardini[a]

[a]Unit of Histology and [b]Division of Pharmacology, Department of Clinical and Experimental Medicine, University of Pisa, Pisa, Italy
[c]Unit of Human Anatomy and Histology, Department of Basic Medical Sciences, Neurosciences and Sensory Organs, School of Medicine, University of Bari, Bari, Italy
[d]Unit of General Surgery, [e]Unit of Pathology, University Hospital, Pisa, Italy
[f]Gastroenterology and Hepatology Section, Department of Medicine, University of Perugia, Perugia, Italy
[g]Second Section of Pathology, Spedali Civili, Brescia, Italy

Corresponding Author:
Nunzia Bernardini, MD
Unit of Histology
Department of Clinical and Experimental Medicine
University of Pisa
Via Roma, 55
I-56126 Pisa, Italy
e-mail: nunzia.bernardini@med.unipi.it

Key Words: ulcerative colitis, active disease, colonic muscle remodelling, intestinal angiogenesis, intestinal fibrosis

Short title: Tissue remodelling in UC

Abbreviations: ECM, extracellular matrix; IBD, inflammatory bowel disease; LL-UC, long-lasting ulcerative colitis; PCNA, proliferating cellular nuclear antigen; SL-UC, short-lasting ulcerative colitis; α-SMA, alpha-smooth muscle actin; SMCs, smooth muscle cells

Manuscript Doi : 10.1093/ecco-jcc/jjw076

Abstract

Background and Aims: Intestinal fibrosis is a complication of inflammatory bowel disease (IBD). Although fibrostenosis is a rare event in ulcerative colitis (UC), there is evidence that a fibrotic rearrangement of colon occurs in the later stages. This is a retrospective study aimed at examining the histopathological features of colonic wall in both short-lasting (SL) and long-lasting (LL) UC.

Methods: Surgical samples of left colon from non-stenotic SL (≤ 3 years, n=9) and LL (≥ 10 years, n=10) UC patients with active disease were compared to control colonic tissues from cancer patients without UC (n=12) to assess: collagen and elastic fibers by histochemistry; vascular networks (CD31/CD105/nestin) by immunofluorescence; parameters of fibrosis [type I and III collagen, fibronectin, RhoA, alpha-smooth muscle actin (α-SMA), desmin, vimentin] and proliferation [proliferating nuclear antigen (PCNA)] by Western blot and/or immunolabelling.

Results: Colonic tissue from both SL-UC and LL-UC showed *tunica muscularis* thickening and transmural activated neovessels (displaying both proliferating CD105-positive endothelial cells and activated nestin-positive pericytes), as compared to controls. In LL-UC the increased collagen deposition was associated with an up-regulation of tissue fibrotic markers (collagen I and III, fibronectin, vimentin, RhoA), an enhancement of proliferation (PCNA) and, along with a loss of elastic fibers, a rearrangement of the *tunica muscularis* towards a fibrotic phenotype.

Conclusions: A significant transmural fibrotic thickening occurs in colonic tissue from LL-UC, together with a cellular fibrotic switch in the *tunica muscularis*. A full-thickness angiogenesis is also evident in both SL- and LL-UC with active disease, as compared to controls.

Manuscript Doi : 10.1093/ecco-jcc/jjw076

INTRODUCTION

Ulcerative colitis (UC) is a chronic inflammatory bowel disease (IBD) with an increasing incidence in western countries, associated with different degree of short/long-term disabilities due to intestinal dysmotility and symptoms such as abdominal pain, diarrhoea, and altered evacuation.[1,2] Althought the etiology of UC is unknown, it results from a dysregulated immune response with tissue damage occurring in the large bowel, with complications that are increasingly attracting the interest of researchers and clinicians.[3,4,5,6]

In the setting of chronic intestinal inflammation, abnormal tissue repair may occur, and lead to intestinal fibrosis and strictures with consequent serious clinical problems, which affect mainly Crohn's disease patients. Intestinal fibrosis is viewed as a long-lasting healing process of the gut that results from both an increased and altered deposition of extracellular matrix (ECM) together with a reduced breakdown of ECM components.[4,7] These fibrotic rearrangements have been largely overlooked in UC, since it is acknowledged as an inflammatory disease confined to the mucosal/submucosal layers, which can develop strictures infrequently (1-10%), as compared to Crohn's disease.[8,7] Not surprisingly, besides muscular hypertrophy, regarded as responsible for the development of strictures in UC, a consistent fibrotic deposition has been reported also in UC: in particular, a transmural collagen enhancement has been demonstrated in UC,[9] regardless of disease duration.[10]

When considering the cellular components that contribute to fibrogenesis in the inflamed bowel, recent studies suggest the involvement of smooth muscle cells (SMCs) and cells of vascular origin.[11,12,13,14] In particular, in the setting of bowel inflammation, the occurrence of endothelial-to-mesenchymal transition has been described as a novel mechanism of intestinal fibrosis, thus suggesting that collagen-producing cells may stem also from transformation of non-mesenchymal cells.[14,15]

Although strictures are known to affect low proportions of UC patients, usually over the course of long-standing disease, considering the important clinical consequences of colonic fibrotic deposition even in the absence of strictures, histopathological studies in non-stenotic UC during the time-course of the disease are highly expected.[7]

Based on the above background, the present study was designed to evaluate whether histological and molecular signs of fibrotic and vascular remodelling can be documented in the inflamed colonic wall of patients with short-lasting (SL) and long-lasting (LL) UC, without clinical evidence of obstruction related to strictures.

PATIENTS AND METHODS

Patients selection

Full-thickness samples of left (descending and sigmoid) colon were retrieved from UC patients with active, pharmacologically unresponsive disease, without clinical symptoms of fibrostenosis, who had undergone elective bowel resection due to a severe exacerbation of colitis. Based on the disease duration after the UC diagnosis (colectomy within 3 years or after 10 years), patients were allocated to two subgroups, designated as SL (n=9, 6 males and 3 females, age range 22-74 years) and LL (n=10, 5 males and 5 females, age range 41-77 years) UC. The following clinical and pathological criteria were assessed for each subgroup: mean disease duration; disease extension (ulcerative proctitis, left-sided UC, extensive UC); histological inflammation grade, estimated by the Geboes' score as descripted below; clinical symptoms (stool frequency, rectal bleeding and abdominal pain). Stool frequency was assessed in accordance with the grading of Sutherland and Martin[16] : 0= normal; 1= 1-2 stools/day>normal, 2= 3-4 stools/day>normal, 3= >4 stools/day>normal. Control colonic samples were obtained from 12 subjects (7 males, 5 females; age range 37–73 years), who underwent elective surgery for uncomplicated left colon cancer, without previous history of abdominal surgery, inflammatory bowel disease or intestinal

obstruction. Specimens, including teniae, were taken at least 5 cm far from resection margins in tumour free areas. The selection of UC and control patients was based on the availability of both frozen and paraffin-embedded colonic tissues archived in the pathology tissue bank. Since the study was performed on archival material, no individual patient identification was involved, and no study-driven clinical intervention was performed. Accordingly, a simplified procedure for Institutional Review Board approval was followed.

Histological evaluation

Full-thickness colonic samples, formalin-fixed and paraffin-embedded, were serially cross-sectioned (3 μm-thickness) for each patient. Then, sections were deparaffinized, rehydrated and processed for routine haematoxylin/eosin (H&E) staining, histochemical staining for collagen and elastic fibers, and immunostaining as follows.

Histopathology. Inflammatory lesions were scored in accordance with previously described histopathological criteria.[17,18] In particular, the Geboes' microscopic score was employed to estimate the severity and inflammatory activity of UC by evaluation of: structural tissue damage; chronic inflammatory infiltrate; presence of eosinophils and/or neutrophils in the *lamina propria*/epithelium; crypt destruction; erosions/ulcerations. The score, with values ranging from 0 (no inflammation) to 22 (maximum inflammation), was determined on colonic slices in the most involved region.

Histochemistry. Tissue collagen and elastic fiber deposition were evaluated by Sirius Red/Fast Green and orcein, as previously reported.[19,20]

Immunoperoxidase. Slides were incubated overnight at 4°C with primary antibodies, with the purpose of detecting matrix fibers by rabbit anti-type I and III collagen ([1:1000]; code: ab34710 and ab7778, respectively, Abcam, Cambridge, UK) and rabbit anti-fibronectin ([1:10000]; code: 1574-1, Epitomics, Burlingame, CA, USA. They were then exposed to biotinylated immunoglobulins (goat anti-rabbit and anti-mouse ([1:200]; code: BA-1000 and BA-9200,

respectively, Vector Lab, Burlingame, USA), peroxidase-labelled streptavidin complex, and 3.3'-diaminobenzidine tetrahydrochloride (DakoCytomation, Glostrup, Denmark), as previously described.[21] Sections were examinated by a Leica DMRB light microscope, and representative photomicrographs were taken by a DFC480 digital camera (Leica Microsystems, Cambridge, UK).

Immunofluorescence. Double immunolabellings, carried out with cell-specific and proliferation markers were analysed by confocal microscopy immunofluorescence. CD31/PECAM-1 and von Willebrand factor (vWF) were used as markers of endothelial cells; CD105/endoglin as a marker of activated/proliferating endothelial cells; nestin for activated pericytes/mural cells; alpha-smooth muscle actin (α-SMA) to identify SMCs; proliferating cellular nuclear antigen (PCNA) for identifying proliferating cells; cytoskeleton filaments, desmin and vimentin as markers of cell phenotype. The primary antibodies were as follows: mouse anti-CD31 ([1:25]; code: M0823, DakoCytomation), rabbit anti-CD105 ([prediluted]; code: ab27422, Abcam), mouse anti-nestin ([1:400]; code: MAB353, Millipore, Billerica, USA), rabbit anti-vWF ([1:400]; code: Ab6994, Abcam), mouse anti-PCNA ([1:1000]; Santa Cruz Biotechnology, Inc., Heidelberg, Germany) mouse anti-α-SMA ([ready to use] code: 760-2833, Cell Marque, Rocklin, CA, USA), rabbit anti-desmin ([1:500]; code: ab8592, Abcam), rabbit anti-vimentin ([1:1000]; code: ab92547, Abcam). Briefly, sections were sequentially incubated with: 0.5% Triton X-100 (Merck KGaA, Darmstadt, Germany) in PBS solution, Protein Block Serum Free (DakoCytomation), combined primary antibodies diluted in PBS (overnight at 4°C), revealed by appropriate fluorophore-conjugated secondary antibodies (goat anti-mouse Alexa 488 and goat anti-rabbit Alexa 568 ([1:300]; code: A-11029 and A-11011, respectively; Invitrogen, Eugene, USA) or biotinylated secondary antibody (biotinylated goat anti-mouse ([1:200]; code: BA-9200, Vector) followed by Alexa 488 conjugated streptavidin ([1:300]; code: S-32354; Invitrogen) followed by nuclear counterstaining with TO-PRO3 (Invitrogen). Stainings were examined under a Leica TCS SP5 confocal laser-scanning microscope (Leica Microsystems, Mannheim, Germany) using a sequential scan procedure.

Confocal images were taken at 250-500 nm intervals through the z-axis of sections, by means of 40x and 63x oil lenses. Z-stacks of serial optical planes were analyzed by confocal software (Multicolor Package; Leica Microsystems) as previously described.[22] Negative controls were prepared by omitting the primary antibodies, pre-adsorbing the primary antibodies with an excess of antigen when available, and mismatching the secondary antibodies.

Vessel quantification. The amount of vessels was calculated by laser confocal microscopy using a computer-aided morphometric analysis with the Leica confocal Multicolor Package and ImageJ software (NIH, Bethesda, MA, USA). In order to detect vessel profiles from the distributions of CD31-positive pixels, only gaps in the stains wider than 2.0 µm were considered to be lumens, and only stained objects in the range 4.5 µm to 15 µm wide were considered to be microvessels. Microvessel density was calculated considering the percentage area of vessels, which was calculated taking into account the total vessel area fraction, lumina included, on the total image area, together with the cumulative vessel length (100µm/volume of scanned tissue normalized to $10^6 \mu m^3$).[23]

Western blot analysis in colonic tissues

After thawing, full-thickness colonic specimens were dissected to separate mucosa from muscle layers and then lysed in RIPA buffer. Homogenates were spun by centrifugation at 20,000 revolutions/min for 15 min at 4°C, and the resulting supernatants were then separated from pellets and stored at -20°C. Protein concentration was determined in each sample by the Bradford method (Protein Assay Kit; Bio-Rad Laboratories, Hercules, CA). Aliquots of 30 µg of protein were separated by electrophoresis on 8% SDS-polyacrylamide gel electrophoresis and transferred onto a poly(vinylidene difluoride) membrane. The blots were then blocked for 1 h with appropriate buffer and incubated overnight at room temperature with the following primary antibodies: rabbit anti-type I and III collagen ([1:5000]; Abcam); rabbit anti-fibronectin ([1:10000]; Epitomics); rabbit anti-SMA ([1:1000]; code: ab5694, Abcam); rabbit anti-vimentin ([1:1000]; Abcam); mouse anti-PCNA

([1:1000]; Santa Cruz), and rabbit anti-RhoA ([1:1000]; code ARH03, Cytoskeleton, Denver, CO, USA). After repeated washings with TBS-T, a goat anti-rabbit and anti-mouse peroxidase-conjugated secondary antibody ([1:10000]; code: sc2004 and sc2005, respectively, Santa Cruz) was added for 1 h at room temperature. After repeated washings with TBS-T, immunoreactive bands were visualized by incubation with chemiluminescent reagents (Immobilon reagent; Millipore Corporation, Billerica, MA) and exposed to Eastman Kodak (Rochester, NY) Image Station 440 for signal and densitometric image analysis. To ensure equal loading and accuracy of changes in protein amount, protein levels were normalized to β-actin.

Image Analysis and Statistics

Two blind pathologists/histologists quantitatively estimated the inflammatory lesions (DC and MC), histochemical data (CS and CI) and vessel density (FG and ME), analyzing the same samples by the same standardized procedures of all tissue specimens under study; the respective values were then averaged and plotted in graphs as previously reported.[21,20] Briefly, for each patient, microscopic fields captured from 3 non-adjacent sections were analyzed and evaluated by the Image Analysis System "L.A.S. software v.4". Positive areas were expressed as percentage of the total tissue area examined (percentage positive pixels [PPP]). Data were expressed as mean ± SEM, statistically analysed using one-way ANOVA followed by the appropriate post hoc test (Bonferroni's test) or, when required, Student's t-test for unpaired data (two tailed). Statistical significance was set at $P \leq 0.05$.

RESULTS

The two subgroups of patients, affected by SL-UC and LL-UC, did not differ significantly in terms of disease location, clinical symptoms and treatments (Table 1).

Histopathology

All UC specimens displayed typical UC mucosal/submucosal lesions, inflammatory infiltration, erosion/ulceration and crypt destruction: a high Geboes' score was obtained for both SL-UC and LL-UC (19.33±1.26 and 21.17±0.40, respectively), without significant differences. A significant thickening of *tunica muscularis* was observed in all UC patients, with a 1.2- and 1.32-fold increase in SL-UC and LL-UC, respectively, *versus* controls (1948.42±39.44 µm and 2060.03±80.06 µm, respectively, *versus* 1558.34±63.33, P≤0.01) (Fig. 1). Conversely, normal morphological patterns were detected in colonic samples from all control subjects, with an intact mucosal layer, occasional inflammatory cells, and a well preserved *tunica submucosa* and *muscularis* (Fig. 1).

When examining colonic blood vessels, an increased network was observed in all layers of both SL-UC and LL-UC samples, as compared with control subjects (Fig. 2). Inflamed tissues displayed a higher density of microvessels lined by CD31-positive/CD105-positive activated endothelial cells as well as a network of highly CD31-positive very small vessels (Fig. 2). Notably, microvessels of the inflamed colon displayed several proliferating endothelial cells with PCNA-positive nuclei as well as activation of pericytes/mural cells, which were found to overexpress nestin (Fig. 2). The highest increase in vessel density was detected in the *tunica muscularis* of inflamed colon in both SL-UC and LL-UC, which displayed a fold increase of 9.6 and 5.8 *versus* controls, respectively (Table 2).

Fibrotic changes in UC

Sirius Red-positive collagen fibers were significantly increased in LL-UC, reaching the overall amount of 46.42±3.72 (P≤0.001) in the whole colonic wall, as compared to controls (27.41±2.14) and SL-UC (29.89± 0.89). When examining separately the colonic layers, collagen deposition in LL-UC was 1.5 folds higher in the *tunica mucosa/submucosa* and 1.7 folds in the *tunica muscularis* than in controls, and 1.5 folds higher in the *tunica mucosa/submucosa* and 1.4

folds in the *tunica muscularis* than in SL-UC (Fig. 3). By contrast, orcein-positive elastic fibers were significantly reduced in LL-UC displaying a 0.5-fold decrease *versus* controls (Fig. 4).

Molecular data showed a significant increase in type I and III collagens and fibronectin, within the mucosal and muscle layers, in LL-UC samples as compared to both controls and SL-UC. In particular, increased collagen I and III immunostaining was observed at level of the outer layers of longitudinal muscle (i.e., serosal side), along which it was arranged as bunches of fibers intermingled with bundles of SMCs. Large amounts of fibronectin were found mainly within the circular muscle and along the myenteric ridge (Fig. 5).

Wall remodelling in longstanding UC

Further studies were focused on tissue and molecular rearrangement of the inflamed colonic wall from patients with LL-UC, which resulted more compromised in terms of fibrotic deposition as compared with SL-UC. The inflamed *tunica muscularis* displayed a significant enhancement of collagen type I and III, fibronectin, RhoA, PCNA as well as vimentin, the latter being increased also in the mucosa (Fig. 5 and 6). By contrast, in LL-UC patients we observed a significant fall in α-SMA expression in both the colonic mucosa and *tunica muscularis* (Fig. 6). Immunofluorescence studies on the *tunica muscularis* showed SMCs displaying an uneven α-SMA staining pattern and absence of desmin as well as many vimentin-positive cells; PCNA-positive nuclei were strongly stained in several vimentin-positive cells and faintly stained in few α-SMA-positive cells (Fig. 7).

DISCUSSION

In the present study, we report original findings concerning the comparative analysis of histopathologic and molecular alterations occurring in full-thickness colonic specimens of UC patients affected by SL and LL active disease, thus providing new insights into the tissue and molecular rearrangement of the inflamed colonic wall at different stages of UC. In particular, an overall view of our observations indicates that the two subgroups of UC patients displayed two

main distinctive features in their inflamed colonic tissues: 1) an increased density of neovessels that was evident in both subgroups, although with a significant predominance in SL-UC; 2) a significant increase in fibrotic deposition that occurred in LL-UC, but not in SL-UC.

In our series, the first original finding regards the evidence that, at variance with previous studies, which documented the occurrence of angiogenesis in the UC mucosa,[24,25] the increase in vascular density was observed as a full-thickness process in both SL- and LL-UC. Of interest, the district most affected by angiogenesis was the muscle layer, where the increase in vasculature achieved fold-increments of 9.6 and 5.8 in SL- and LL-UC, respectively, as compared to non-inflamed control tissues. In agreement with the morphometric analysis, the neovessels observed in the inflamed colon showed several signs of activation, such as the presence of proliferating CD105/PCNA-positive endothelial cells as well as activated nestin-positive pericytes. Moreover, the evidence that the intense network of proliferating microvessels was detected in both UC subgroups suggests that it is likely related with the severity of inflammatory activity rather than disease duration. Indeed, angiogenesis is regarded as a hallmark of active intestinal inflammation, closely related to disease severity, and invariably described in the inflamed bowel mucosa.[26,27,28] In recent years, angiogenesis has gained considerable attention in the pathogenesis of IBD, being considered a crucial event in the initiation and progression of bowel inflammation.[15] However, scarce data are currently available on the histological rearrangements of microvessel architecture throughout the different layers of the inflamed bowel wall in UC patients. Only when considering the colonic mucosa, elegant studies have shown that it is endowed with potent angiogenic activity in UC patients,[24] and that in animal models of colitis a correlation exists between tissue injury and the inflammation-driven mucosal angiogenesis.[25]

With regard to collagen and fibronectin evaluations, we observed significant fibrotic deposition throughout the whole thickness of the left colon in LL-UC patients, while only a trend towards transmural fibrosis was found in SL-UC. These findings are partly consistent with the

fibrotic rearrangement of colonic wall reported in both preclinical models of colitis and UC patients, even though some differences can be recognized, depending on the disease activity, extension, duration and degree of fibrotic remodelling. In particular, transmural collagen deposition has been recently described in experimental models of colitis[12,19,29,30,31] as well as in UC patients with advanced fibrotic disease.[32] De Bruyn et al.[10] observed increased full-thickness amounts of collagen in the colon of UC patients with both early (< 2 years, with active inflammation) and longstanding (> 10 years, without inflammatory activity) disease, without any significant change in collagen expression over the time.

Of interest, besides the increased levels of collagen type I-III and fibronectin, detected in both mucosal and muscle layers of LL-UC, we found also an up-regulation of collagen type III in the mucosa of SL-UC, this observation being consistent with the condition of active colonic inflammation and the high ratio of type III:I collagen described previously in the submucosa of UC patients.[9] Moreover, when considering the increased transmural deposition of fibronectin that we observed in LL-UC patients, it is worth mentioning that a similar finding has been reported previously for the intestinal fibrosis associated with Crohn's disease[33] and, more recently, for the colonic mucosa of LL-UC in the absence of inflammatory activity.[10]

In the present work, another original finding was the loss of elastic fibers observed throughout the full-thickness of the inflamed colonic wall in LL-UC, but not SL-UC, patients. Due to the mechanical properties of elastin, that allows tissues to recoil after repeated stretching, the reduced presence of elastic fibers may result in defects of the elastic properties of bowel wall, thus contributing to worsen further the condition of bowel dysmotility that occurs often in IBD and is thought to be primarily associated with alterations of neuromuscular cell components.[21,32,34,35,36]

Although UC is known to evolve towards fibrostenosis with much lower frequency than Crohn's disease (1-10%), particularly in patients with long-lasting disease,[8,11,37] with important clinical consequences, such as severe bowel dysmotility,[6,38,] it is important to consider that fibrotic

strictures result from slow-rate processes, supported by chronic inflammation and long-lasting tissue remodelling. On this basis, we deemed it interesting to focus the second part of this study on LL-UC, which was found to be mostly affected by collagen deposition and loss of elastic fibers, in order to examine whether molecular and cellular colonic remodelling occur in the advanced stages of disease.

At level of the *tunica muscularis,* in addition to increments of collagens and fibronectin, in the inflamed colon of LL-UC patients we detected an upregulation of vimentin, a decrease in α-SMA and desmin, along with abundant proliferating PCNA-positive cells, as compared to non-inflamed controls. Interestingly, we observed a diffuse phenotype modulation of cells within the *tunica muscularis*. In particular, the quiescent, non-proliferative (PCNA-negative) smooth muscle cell phenotype (α-SMA-positive/desmin-positive/vimentin-negative) was replaced by proliferative myofibroblast-like (reduced, deranged α-SMA/desmin-negative/vimentin-negative) and several proliferative fibroblast-like (α-SMA-negative/desmin-negative/vimentin-positive) phenotypes. In keeping with data reported by *in vitro* and *in vivo* studies on enteric muscle layers in experimental colitis, [12,13,19] the fibrogenic phenotypic rearrangement, as observed in the present study, provides evidence in humans that, under inflammatory conditions, the *tunica muscularis* undergoes a cellular fibrotic switch, which, along with collagen deposition and elastin loss, may contribute to impairments of its motor functions. Interestingly, insightful observations, made in *in vitro* studies, suggest that stiffness of intestinal tissues can trigger morphological and functional changes in human colonic fibroblasts and myofibroblasts, from a non-proliferative to an activated fibrogenic myofibroblast phenotype.[39,40] In this light, a stiff ECM could be considered not as a result, but rather as a source of tissue fibrosis in IBD, with a critical role in supporting the development and progression of fibrogenesis.

Our data on the fibrotic switch of inflamed smooth muscle in LL-UC are strengthened by the finding of an up-regulation of RhoA expression in muscle layers. Indeed, there is consistent

evidence supporting an important role of the Rho/Rho kinase pathway in the determinism of intestinal fibrosis.[41] In particular, RhoA signaling plays a relevant role in the fibrogenic differentiation of intestinal SMCs both in human radiation enteritis[42] and in *in vitro* models of human intestinal fibrogenesis, where novel approaches to antifibrotic strategies have been investigated by pharmacologic modulation of the RhoA pathway.[40] Of interest, the enhancement of tissue RhoA expression, as well as the upregulation of the other molecular factors related to fibrosis (i.e., collagen I and III, fibronectin, vimentin), suggest that critical factors involved in fibrogenesis can be expressed in the advanced phases of the UC disease, also in the absence of evident strictures.

Before moving to the conclusions of this work, we wish to address the issue of the difficulty in comparing data obtained from different clinical studies. In this respect, several variables of heterogeneity of the study populations (e.g., clinical history, histopathological lesions, disease activity and duration) can lead to disparate findings. The different investigated parameters, together with different techniques employed in different laboratories, can complicate the picture further. In addition, when performing retrospective investigations, as the present one, some important limitations depend on the availability of tissue samples, as previously reported.[9] In particular, in the present study the selection of tissue specimens was made on the basis of the availability, for each patient, of both frozen and paraffin-embedded samples of the left colon, this limiting the choice of samples for our assays.

In summary, the results of the present study indicate that an intense transmural vessel growth occurs in both SL- and LL-UC patients with active disease. In LL-UC patients, besides significant signs of fibrosis throughout the whole thickness of colonic wall and loss of elastic fibers, we observed a fibrotic switch of the *tunica muscularis*, which reduces its muscle features and acquires proliferative phenotypes.

Acknowledgment
This work was supported by an institutional research grant issued by the Interdepartmental Center for Research in Clinical Pharmacology and Experimental Therapeutics, University of Pisa, Italy. The authors are very grateful to Mr. Sauro Dini for his skillful technical assistance in histological preparation and staining.

Conflict of interest
The authors confirm that they have no conflicts of interest.

Authors' contributions to the work described in the manuscript
Design of the study (NB, CB, DV), sample and reagent supplies (PB, GDC, DC, MC), performing experiments (CI, CS, RC, ET, ME, FG), data acquisition and analysis (CI, CS, RC, ET, ME, FG, DC, MC, VV, GB), supervision of the experimental procedures and interpretation of data (NB, CB, AD, DV), drafting the paper (NB, CI)

Ethical approval
All applicable international, national, and/or institutional guidelines for the care and use of animals were followed.

REFERENCES

1. Busch K, Sonnenberg A, Bansback N. Impact of inflammatory bowel disease on disability. *Curr Gastroenterol Rep* 2014;**16**:414.

2. Haase AM, Gregersen T, Christensen LA, *et al*. Regional gastrointestinal transit times in severe ulcerative colitis. *Neurogastroenterol Motil* 2016;**28**:217-24. doi: 10.1111/nmo.12713. Epub 2016 Jan 4.

3. Khor B, Gardet A, Xavier RJ. Genetics and pathogenesis of inflammatory bowel disease. *Nature* 2011;**474**:307-17.

4. Rieder F, de Bruyn JR, Pham BT, *et al.* Results of the 4th scientific workshop of the ECCO (Group II): markers of intestinal fibrosis in inflammatory bowel disease. *J Crohns Colitis* 2014;**8**:1166-78.

5. Latella G, Rogler G, Bamias *G, et al.* Results of the 4th scientific workshop of the ECCO (I): Pathophysiology of intestinal fibrosis in IBD. *J Crohns Colitis* 2014**;8**:1147-65.

6. D'Haens G, Bressler B, Danese S, Gibson P, Hanauer SB, Sandborn W, The Crohn's Disease–Ulcerative Colitis Clinical Appraisal. *Clin Gastroenterol Hepatol*, 2016; doi: 10.1016/j.cgh.2016.01.017

7. Gordon IO, Agrawal N, Goldblum JR, Fiocchi C, Rieder F. Fibrosis in ulcerative colitis: mechanisms, features, and consequences of a neglected problem. *Inflamm Bowel Dis* 2014;**20**:2198-206.

8. Torres J, Billioud V, Sachar DB, Peyrin-Biroulet L, Colombel JF. Ulcerative colitis as a progressive disease: the forgotten evidence. *Inflamm Bowel Dis* 2012;**18**:1356-63.

9. Lawrance IC, Maxwell L, Doe W. Altered response of intestinal mucosal fibroblasts to profibrogenic cytokines in inflammatory bowel disease. *Inflamm Bowel Dis* 2001;**7**:226-36.

10. de Bruyn JR, Meijer SL, Wildenberg ME, Bemelman WA, van den Brink GR, D'Haens GR. Development of Fibrosis in Acute and Longstanding Ulcerative Colitis. *J Crohns Colitis* 2015;**9**:966-72.

11. Lund PK, Zuniga CC. Intestinal fibrosis in human and experimental inflammatory bowel disease. *Curr Opin Gastroenterol* 2001;**17**:318-23.

12. Marlow SL, Blennerhassett MG. Deficient innervation characterizes intestinal strictures in a rat model of colitis. *Exp Mol Pathol* 2006;**80**:54-66.

13. Nair DG, Han TY, Lourenssen S, Blennerhassett MG. Proliferation modulates intestinal smooth muscle phenotype in vitro and in colitis in vivo. *Am J Physiol Gastrointest Liver Physiol* 2011;**300**:G903-13.

14. Rieder F, Kessler SP, West GA, *et al.* Inflammation-induced endothelial-to-mesenchymal transition: a novel mechanism of intestinal fibrosis. *Am J Pathol* 2011;**179**:2660-73.

15. Cromer WE, Mathis JM, Granger DN, Chaitanya GV, Alexander JS. Role of the endothelium in inflammatory bowel diseases. *World J Gastroentero* 2011**;17**:578-93.

16. Sutherland LR, Martin F. 5-Aminosalicylic acid enemas in treatment of distal ulcerative colitis and proctitis in Canada. *Dig Dis Sci* 1987;**32**:64S-66S.

17. Geboes K, Riddell R, Öst A, Jensfelt B, Persson T, Löfberg R. A reproducible grading scale for histological assessment of inflammation in ulcerative colitis. *Gut* 2000;**47**:404-409.

18. Langner C, Magro F, Driessen A, et al. The histopathological approach to inflammatory bowel disease: a practice guide. *Virchows Arch* 2014;**464**:511-27.

19. Ippolito C, Segnani C, Errede M, *et al.* An integrated assessment of histopathological changes of the enteric neuromuscular compartment in experimental colitis. *J Cell Mol Med* 2015;**19**:485-500.

20. Segnani C, Ippolito C, Antonioli L, *et al*. Histochemical detection of collagen fibers by Sirius Red/Fast Green is more sensitive than van Gieson or Sirius Red alone in normal and inflamed rat colon. PLoS One. 2015;**10**:e0144630. doi: 10.1371/journal.pone.0144630. eCollection 2015.

21. Bernardini N, Segnani C, Ippolito C, *et al.* Immunohistochemical analysis of myenteric ganglia and interstitial cells of Cajal in ulcerative colitis. *J Cell Mol Med* 2012;**16**:318-27.

22. Virgintino D, Errede M, Rizzi M, *et al.* The CXCL12/CXCR4/CXCR7 ligand-receptor system regulates neuro-glio-vascular interactions and vessel growth during human brain development. *J Inherit Metab Dis* 2013;**36**:455-66.

23. Mouton PR, Gokhale AM, Ward NL, West MJ. Stereological length estimation using spherical probes. *J Microsc-Oxford* 2002;**206**:54–64.

24. Danese S, Sans M, de la Motte C, *et al*. Angiogenesis as a novel component of inflammatory bowel disease pathogenesis. *Gastroenterology* 2006;**130**:2060-73.

25. Danese S, Scaldaferri F, Vetrano S, *et al.* Critical role of the CD40-CD40-ligand pathway in regulating mucosal inflammation-driven angiogenesis in inflammatory bowel disease. *Gut* 2007;**56**:1248-56.

26. Hatoum OA, Heidemann J, Binion DG. The intestinal microvasculature as a therapeutic target in inflammatory bowel disease. *Ann N Y Acad Sci* 2006;**1072**:78-97.

27. Pousa ID, Maté J, Gisbert JP. Angiogenesis in inflammatory bowel disease. *Eur J Clin Invest* 2008;**38**:73-81.

28. Knod JL, Crawford K, Dusing M, Collins MH, Chernoguz A, Frischer JS. Angiogenesis and vascular endothelial growth factor-A expression associated with inflammation in pediatric Crohn's disease. *J Gastrointest Surg*. 2015 Nov 3. [Epub ahead of print].

29. Suzuki K, Sun X, Nagata M, *et al.* Analysis of intestinal fibrosis in chronic colitis in mice induced by dextran sulfate sodium. *Pathology international* 2011;**61**:228-38.

30. Zhu MY, Lu YM, Ou YX, Zhang HZ, Chen WX. Dynamic progress of 2,4,6-trinitrobenzene sulfonic acid induced chronic colitis and fibrosis in rat model. *J Digest Dis* 2012;**13**:421-9.

31. Lawrance IC, Rogler G, Bamias G, *et al.* Cellular and molecular mediators of intestinal fibrosis. *J Crohns Colitis* 2015 Nov 2. pii: j.crohns.2014.09.008. [Epub ahead of print].

32. Manetti M, Rosa I, Messerini L, Ibba-Manneschi L. Telocytes are reduced during fibrotic remodelling of the colonic wall in ulcerative colitis. *J Cell Mol Med* 2015;**19**:62-73.

33. Kolachala VL, Bajaj R, Wang L, *et al*. Epithelial-derived fibronectin expression, signaling, and function in intestinal inflammation. *J Biol Chem* 2007;**282**:32965-73.

34. Schemann M, Neunlist M. The human enteric nervous system. *Neurogastroent Motil* 2004;**16**:55-9.

35.Bernardini N, Ippolito C, Segnani C, *et al*. Histopathology in gastrointestinal neuromuscular diseases: methodological and ontological issues. Adv Anat Pathol. 2013;20:17-31.

36. Bassotti G, Villanacci V, Nascimbeni R, *et al.* Enteric neuroglial apoptosis in inflammatory bowel diseases. *J Crohns Colitis* 2009;**3**:264-70.

37. Yamagata M, Mikami T, Tsuruta T, *et al*. Submucosal fibrosis and basic-fibroblast growth factor-positive neutrophils correlate with colonic stenosis in cases of ulcerative colitis. *Digestion* 2011;**84**:12-21.

38. Bassotti G, Antonelli E, Villanacci V, Salemme M, Coppola M, Annese V. Gastrointestinal motility disorders in inflammatory bowel diseases. *World J Gastroentero* 2014;**20**:37-44.

39. Johnson LA, Rodansky ES, Sauder KL, *et al*. Matrix stiffness corresponding to strictured bowel induces a fibrogenic response in human colonic fibroblasts. *Inflamm Bowel Dis* 2013;**19**:891-903.

40. Johnson LA, Rodansky ES, Haak AJ, Larsen SD, Neubig RR, Higgins PDR. Novel Rho/MRTF/SRF inhibitors block matrix-stiffness and tgf-beta-induced fibrogenesis in human colonic myofibroblasts. *Inflamm Bowel Dis* 2014;**20**:154-65.

41. Huang Y, Xiao S, Jiang Q. Role of Rho kinase signal pathway in inflammatory bowel disease. *Int J Clin Exp Med* 2015;**8**:3089-97.

42. Bourgier C, Haydont V, Milliat F, *et al.* Inhibition of Rho kinase modulates radiation induced fibrogenic phenotype in intestinal smooth muscle cells through alteration of the cytoskeleton and connective tissue growth factor expression. *Gut* 2005;**54**:336-43.

Manuscript Doi : 10.1093/ecco-jcc/jjw076

Table 1. Pathologic and clinical characteristics of patients with short-lasting and long-lasting ulcerative colitis

		SL-UC	LL- UC	*P value*
Mean disease duration following diagnosis		1.82±0.32	15.90±2.57	*0.0001*
Extent of colitis	*Ulcerative proctitis*	1/9	1/10	*ns*
	Left-sided UC	3/9	3/10	*ns*
	Extensive UC	5/9	6/10	*ns*
Histological inflammation grade		19.33±1.26	21.17±0.40	*ns*
Clinical symptoms	*Stool frequency*	2 (4/9)	2 (5/10)	*ns*
		3 (5/9)	3 (5/10)	*ns*
	Rectal bleeding	6/9	7/10	*ns*
	Abdominal pain	4/9	5/10	*ns*
Previous medication	*Prednisone*	5/9	7/10	*ns*
	5-ASA	4/9	5/10	*ns*
	Methotrexate	1/9	2/10	*ns*
	Cyclosporin	1/9	3/10	*ns*

SL- and LL-UC, short-lasting and long-lasting ulcerative colitis; 5-ASA, 5-aminosalicylic acid; data are presented as mean ± SEM; significative values, P≤0.05;ns, not significant

Manuscript Doi : 10.1093/ecco-jcc/jjw076

Table 2. Vessel density in the inflamed colon of patients with short-lasting and long-lasting ulcerative colitis

	Control	SL-UC	LL-UC
Vessel fraction area %			
Tunica mucosa/submucosa	6.49±0.46	13.29±0.86[a***]	15.96±1.14[a***]
Tunica muscularis	1.11±0.13	10.62±0.80[a***]	6.45±0.35[a***,b***]
Vessel length/volume			
Tunica mucosa/submucosa	9.13±1.10	18.95±1.74[a***]	16.87±1.20[a***]
Tunica muscularis	5.87±0.68	10.58±0.42[a***]	11.66±0.76[a***]

SL- and LL-UC, short-lasting and long-lasting ulcerative colitis ; [a] vs controls, [b] vs SL-UC, *** P≤0.001

FIGURE LEGENDS

Figure 1. Increased thickness of the inflamed colonic wall in short-lasting (SL) and long-lasting (LL) ulcerative colitis (UC), as compared to control colon. Representative pictures of haematoxylin/eosin-stained samples of full-thickness, cross-sectioned left colon. CM, circular muscle; LM, longitudinal muscle. Scale bar: 200 μm.

Figure 2. Proliferative microvessels in inflamed ulcerative colitis (UC). Confocal microscopy representative images of CD31/CD105, CD105/nestin, and PCNA/vWF double immunolabelling in control colon, short-lasting (SL) and long-lasting (LL) ulcerative colitis (UC). Several CD31/CD105-positive microvessels (v, yellowish fluorescence) together with a number of CD31-positive very small vessels (arrows) are present in both mucosal/submucosal and muscle layers of inflamed colon. In control colon CD31-positive endothelial cells, which do not express any CD105, are found in microvessels (v) of all layers, also within a myenteric ganglionic-like cell (g) arrangement. In SL- and LL-UC colon, numerous microvessels (v) display CD105-positive endothelial cells and nestin-positive pericytes/mural cells (arrows). Note in LL-UC nestin-positive ganglionic cells (g). The control colon shows CD105/nestin-negative microvessels (v), which were revealed by a faint autofluorescence of red cells. In both SL-UC and LL-UC, double staining with the endothelial marker vWF and PCNA shows numerous proliferating endothelial cells (arrows). Scale bar 25 μm.

Figure 3. Increased collagen fibers in inflamed long-lasting (LL) ulcerative colitis (UC). Representative photomicrographs of full-thickness colon showing the distribution pattern of Sirius Red-stained collagen fibers and Fast Green-stained non-collagen proteins in control colon, SL-UC and LL-UC, with respective quantification, which are expressed as percentage of positive pixels (PPP) calculated on the *tunica mucosa/submucosa* or *tunica muscularis* tissue area examined. Column graphs display the mean values of PPP±SEM; * $P \leq 0.05$; ** $P \leq 0.01$. Scale bars 50μm.

Figure 4. Decreased elastic fibers in inflamed long-lasting (LL) ulcerative colitis (UC). Representative pictures of the distribution pattern of orcein-stained elastic fibers, in control colon, short-lasting (SL) and long-lasting (LL) UC, with respective quantification, which are expressed as percentage of positive pixels (PPP) calculated on the colonic whole wall tissue area examined. Column graph displays the mean values of PPP±SEM; **P≤0.01; ***P≤0.001. Scale bars: 50μm

Figure 5. Increase in collagen type I and III and fibronectin in inflamed long-lasting (LL) ulcerative colitis (UC). Densitometric analysis of their expression in colonic mucosa and muscle layers taken from control subjects or patients with short-lasting (SL) and LL-UC (left panel), and representative examples of respective immunostaining of full-thickness left colonic slices (right panel). Each column represents the mean±SEM for n=5; *P≤0.05. Scale bars: 50μm.

Figure 6. Fibrotic markers in the inflamed colon of long-lasting (LL) ulcerative colitis (UC). Representative Western blots showing the expression of α–SMA, vimentin, PCNA, RhoA and β-actin and the respective densitometric analysis in colonic mucosa and muscle layers taken from control subjects or LL-UC patients. Each column represents the mean±SEM for n=5; *P≤0.05.

Figure 7. Fibrotic features of the *tunica muscularis* in the inflamed colon of long-lasting (LL) ulcerative colitis (UC). Confocal microscopy representative images of colonic samples double immunostained for α–SMA/desmin or vimentin, and PCNA/vimentin or α–SMA. In UC colon the *tunica muscularis* shows a decrease in desmin content, better highlighted by the single channel (red) shown in the inset, an increment in vimentin-positive cells (inset) with several intensely PCNA-stained nuclei (arrows), and faintly PCNA-stained nuclei in α–SMA-positive cells (arrows). Scale bars: 25 μm (α–SMA/desmin or vimentin), 50 μm (PCNA/vimentin or α–SMA).

Manuscript Doi : 10.1093/ecco-jcc/jjw076

Figure 1

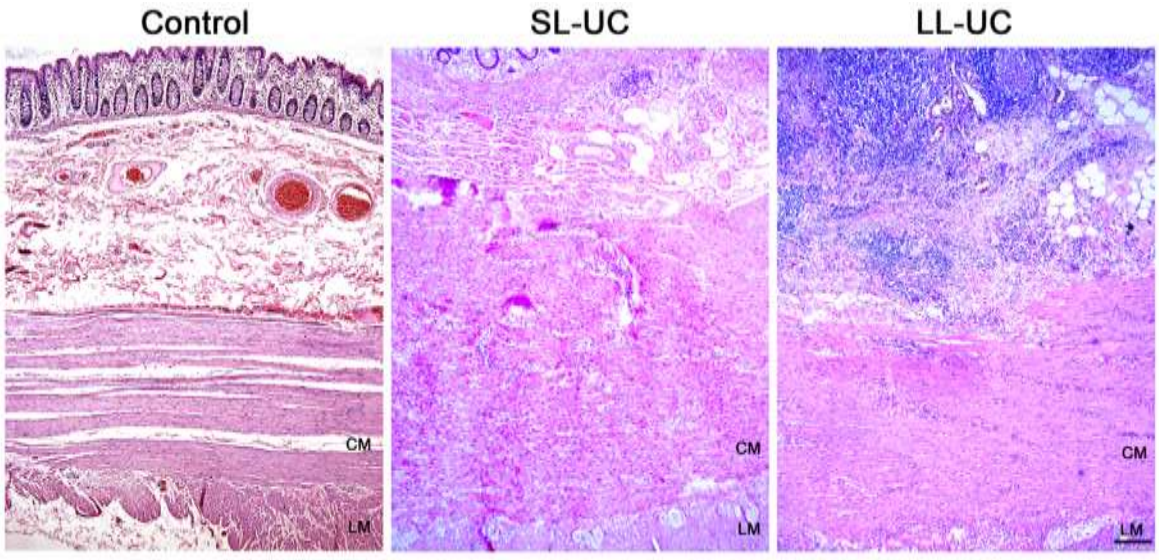

Manuscript Doi : 10.1093/ecco-jcc/jjw076

Figure 2

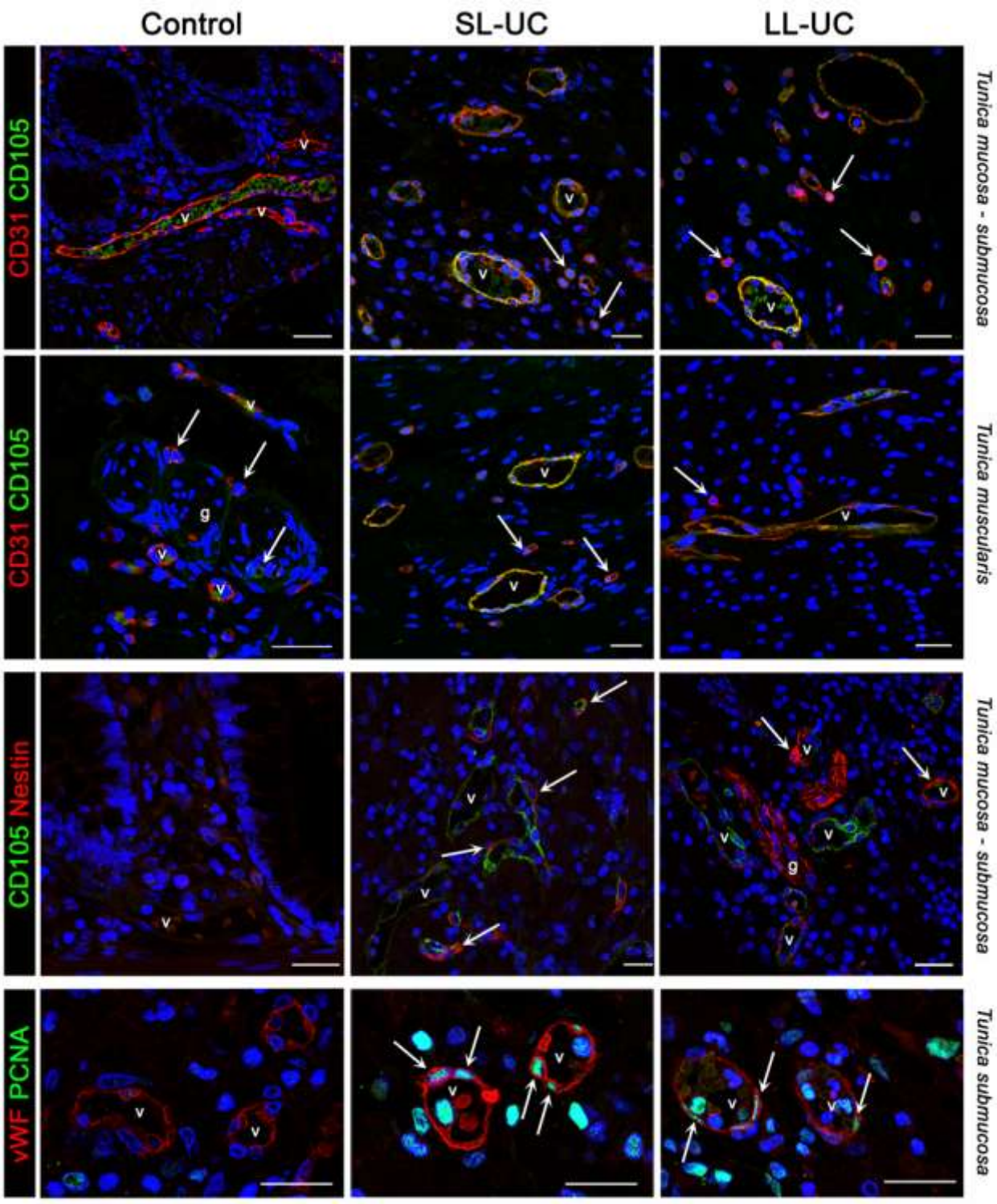

Manuscript Doi : 10.1093/ecco-jcc/jjw076

Figure 3

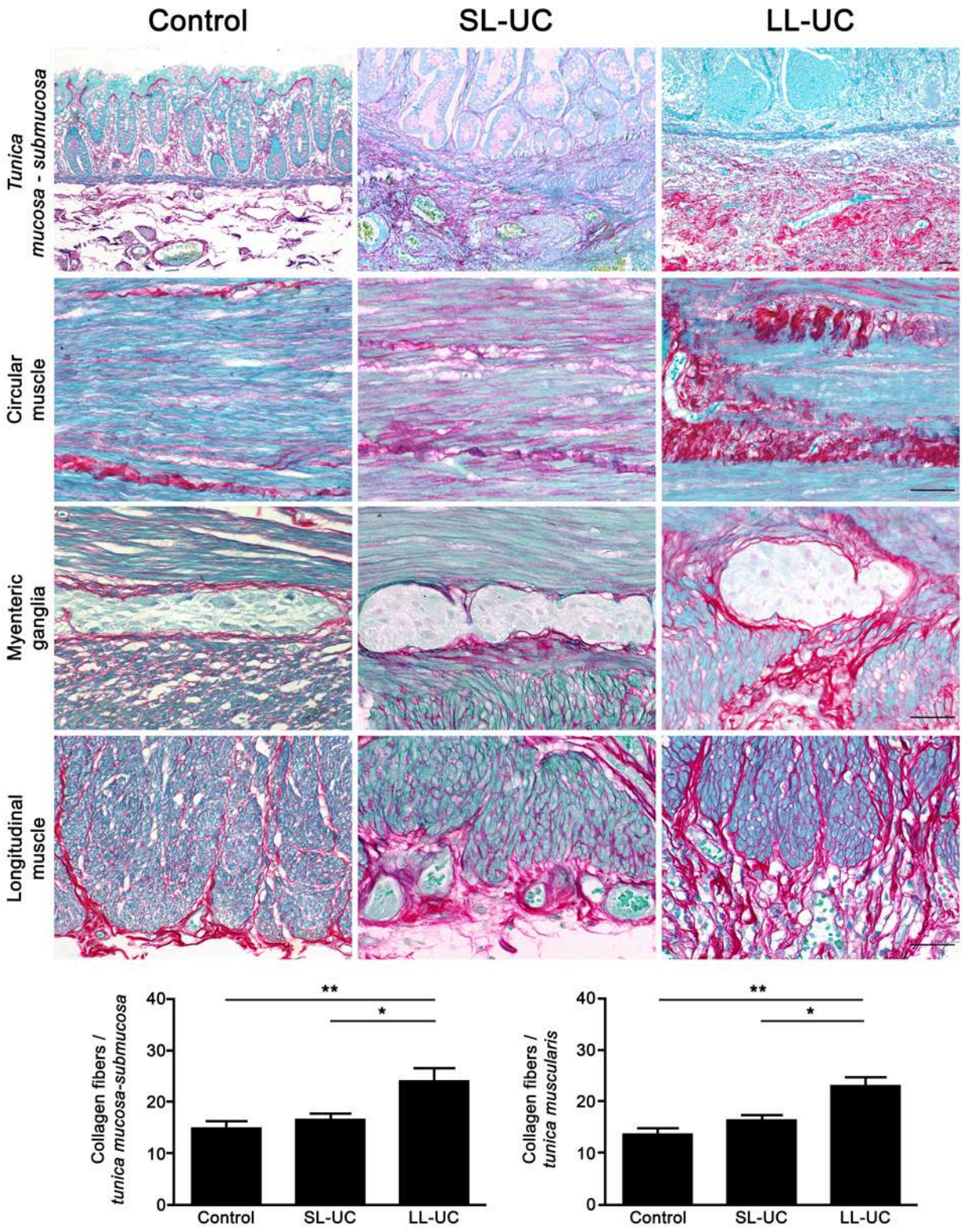

Manuscript Doi : 10.1093/ecco-jcc/jjw076

Figure 4

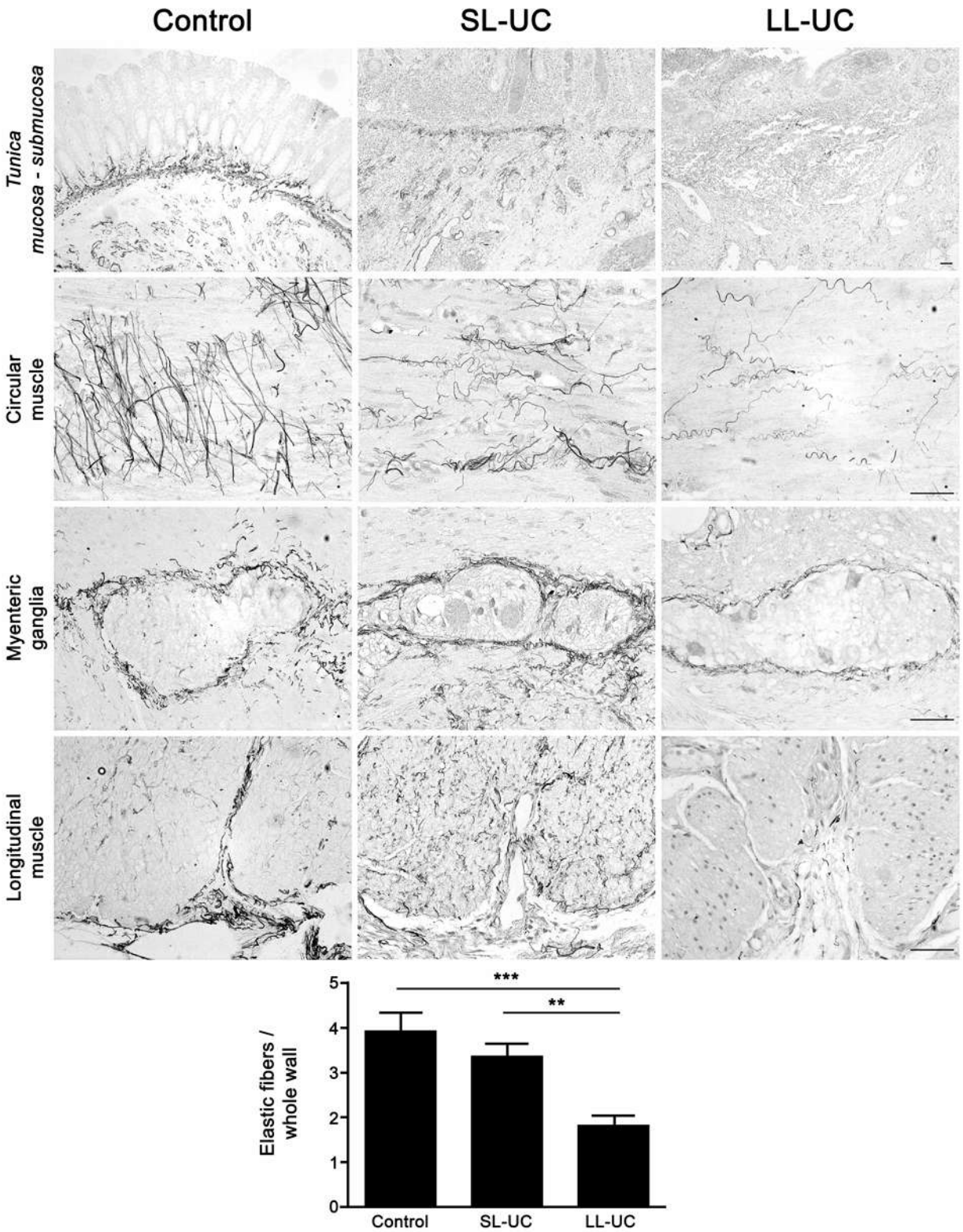

Manuscript Doi : 10.1093/ecco-jcc/jjw076

Figure 5

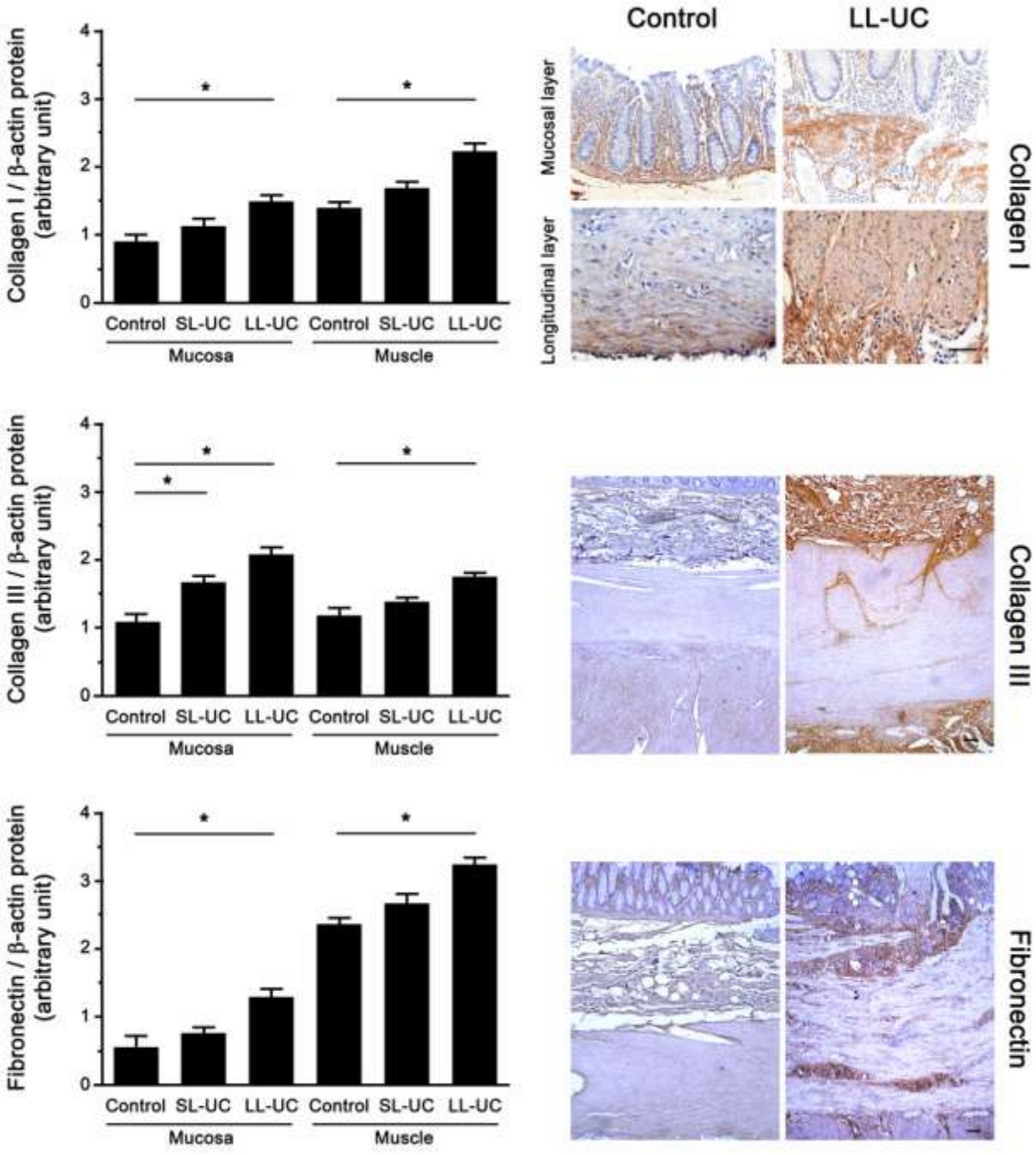

Manuscript Doi : 10.1093/ecco-jcc/jjw076

Figure 6

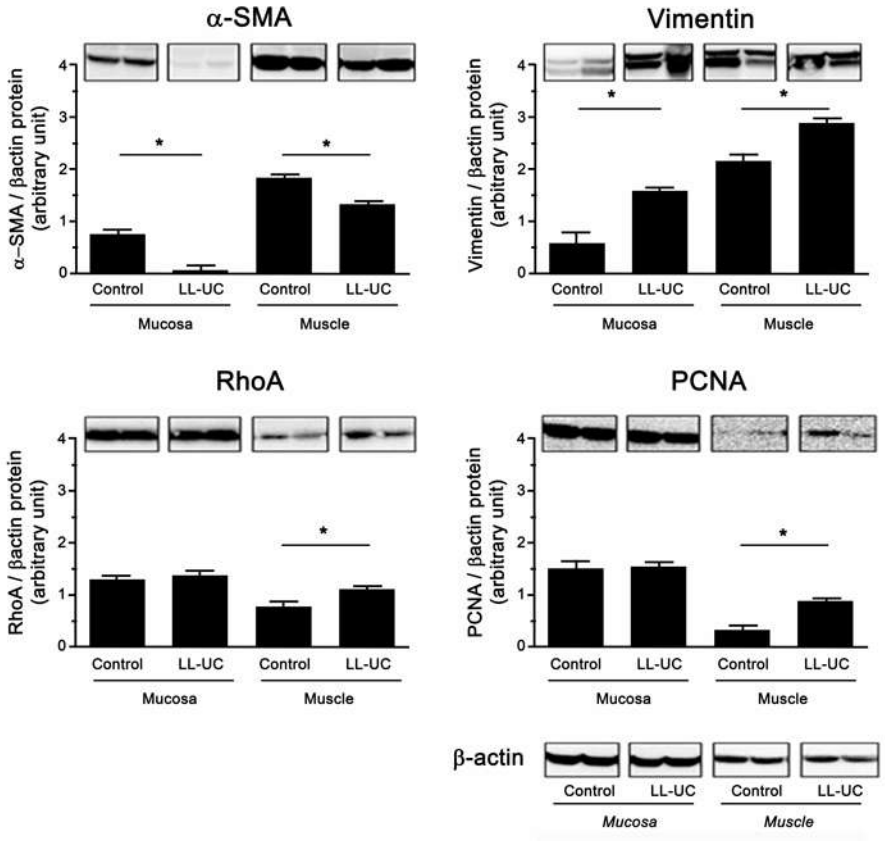

Manuscript Doi : 10.1093/ecco-jcc/jjw076

Figure 7